vibration

MDPI

*Article*

# Seismic Assessment of an Existing Precast Reinforced Concrete Industrial Hall Based on the Full-Scale Tests of Joints—A Case Study

**Biljana Mladenović [1], Andrija Zorić [1], Dragan Zlatkov [1,†], Danilo Ristic [2,†], Jelena Ristic [3], Katarina Slavković [4] and Bojan Milošević [5,*]**

1 Faculty of Civil Engineering and Architecture, University of Niš, 18000 Niš, Serbia
2 Institute of Earthquake Engineering and Engineering Seismology (IZIIS), 1000 Skopje, North Macedonia
3 RESIN Laboratory of Industrial Sciences and Technologies, 1000 Skopje, North Macedonia
4 National Institute of the Republic of Serbia, Mathematical Institute of the Serbian Academy of Sciences and Arts, 11000 Belgrade, Serbia
5 Faculty of Mechanical Engineering and Civil Engineering in Kraljevo, University of Kragujevac, 36000 Kraljevo, Serbia
* Correspondence: milosevic.b@mfkv.kg.ac.rs
† Retired author.

**Abstract**

Construction of precast reinforced concrete (PRC) industrial halls in seismically active areas has been increasing in recent decades. As connections are one of the most sensitive and vulnerable zones of PRC structures, there is a need to pay special attention to their investigation and modeling in seismic analysis. Knowing that each PRC system is specific and unique, this study aims to evaluate the actual seismic performances of PRC industrial halls built in the AMONT system, which represent a significant portion of the existing industrial building stock in Italy, the Balkans, and Turkey. As there is a lack of published research data on its specific joints, the results of the quasi-static full-scale experiments carried out up to failure on the models of four characteristic connections are presented. Since the implementation of nonlinear dynamic analysis in everyday engineering practice can be demanding, a simplified model of the structure considering the effects of the connections' stiffness is proposed in this paper. The differences in the roof top displacements between the proposed model and the model with the rigid joints of the analyzed frames are in the range from 16.53% to 66.93%. The values of inter-story drift ratios are larger by 10–100% when the real stiffness of connections is considered, which is above the limit value provided by standard EN 1998-1. These results confirm the necessity of considering the nonlinear behavior and stiffness of connections in precast frame structures when determining displacements, which is particularly important for the verification of the serviceability limit state of structures in seismic regions.

**Keywords:** precast reinforced concrete structure; industrial hall; connections; full-scale tests; nonlinear behavior; stiffness of connections; dynamic analysis



Academic Editor: Evgeny Petrov and Aleksandar Pavic

Received: 16 December 2025
Revised: 14 January 2026
Accepted: 21 January 2026
Published: 23 January 2026



## 1. Introduction

The industrialization of certain regions in the world has caused a sharp increase in the construction of industrial halls, whereby the most common types are precast reinforced concrete (PRC) structures, even in seismically active areas, due to the known advantages such as increased speed of construction, improved quality control due to the member-fabrication

environment, and reduced site formwork and labor. It is particularly important to recognize that in the design phase, industrial halls have to be treated completely separately from other building-type structures. Structural systems of industrial halls differ from other building structures because floor heights are significantly higher, and spans of main roof beams and floor beams are larger than those of ordinary buildings. Due to the large dimensions of industrial halls, almost all prefabricated elements are large in size and weight. Some halls, especially two-storey and multi-storey ones, can be designed for large payloads, and so in the event of an earthquake, due to the large mass, seismic forces of considerable intensity can be generated, which can cause damage or total collapse of buildings. All of those differences, and differences typical for implementation of precast reinforced concrete construction systems, highly contribute to the existence of very different characteristics of dynamic structural response and resulting damage and failure modes under moderate and strong earthquake ground motions.

Although the total number of industrial structures located in earthquake-prone areas is usually limited, their failure may lead to severe social and economic consequences. Past earthquakes clearly demonstrated the vulnerability of precast reinforced concrete (PRC) industrial buildings when seismic resistance was not adequately considered. For instance, during the 1976 Friuli earthquakes in Italy, a large number of industrial buildings suffered extensive damage or collapse due to the absence of seismic design provisions in the adopted PRC systems [1]. Similarly, the 2012 Emilia-Romagna earthquake revealed deficiencies related to inadequate seismic design and construction details of PRC structures, whereas properly designed and detailed buildings generally exhibited satisfactory performance, as reported by post-earthquake investigations [2]. Turkey is one of the most seismically active regions with short earthquake return periods. In recent decades, destructive earthquakes such as the 2020 Elazığ-Sivrice and 2023 Kahramanmaraş events caused significant casualties and structural damage. In PRC industrial halls, the damage was largely due to design and construction inadequacies, and deficiencies in critical joints, particularly hinged column-to-rafter and column-to-foundation connections [3]. Similarly, Japan, prone to frequent earthquakes, reinforced its seismic evaluation and retrofit legislation after the 1995 Kobe earthquake, leading to improved performance of existing RC buildings, as confirmed during the 2011 Tohoku and 2016 Kumamoto earthquakes [4]. These and other past earthquakes [5–10] highlight the need for thorough experimental, numerical, and analytical studies to enhance seismic performance of industrial structures.

Extensive research conducted since the 1980s has led to the development of precast concrete structural systems and detailing solutions suitable for application in regions of high seismic hazard. A comprehensive review of these advances, including code developments and practical applications, is presented in [11], where it was concluded that the use of precast concrete in seismic regions is feasible and can provide satisfactory seismic performance when appropriately designed.

Stability and seismic performance of precast reinforced concrete (PRC) structural systems largely depend on the behavior of their connections, which have been identified as the most vulnerable components based on damage observations from past earthquakes. Consequently, significant experimental and numerical research has been devoted to the study of PRC connections.

These studies have consistently shown that connections in precast structures exhibit semi-rigid behavior rather than idealized pinned or fully rigid behavior. The influence of connection rigidity on the seismic response of precast concrete frames has been investigated within the framework of the European COST C1 project and by several authors who emphasized the need to consider connection rigidity as a design parameter [12,13]. Experimental investigations, including full-scale tests, further contributed to the characterization and

modeling of beam-to-column connections in precast concrete structures [14]. Analytical studies on the behavior of precast reinforced concrete (PRC) beam-to-column connections have led to the development of various modeling approaches, including section-based methods and analytical models for predicting shear resistance and nonlinear response under seismic excitation [15–17]. These studies highlighted significant differences in seismic response between precast and monolithic RC frames, emphasizing the need for nonlinear models specifically tailored for precast systems.

In parallel, extensive experimental research has been conducted on PRC connections, involving both full-scale and scaled specimens, with the aim of improving connection design and calibrating numerical models [18–20]. Based on these experimental results, numerous numerical models have been developed to simulate different types of beam-to-column and slab–beam–column connections, including dowel, hybrid, and mechanical solutions [21–32].

Despite these advances, investigations focusing on the seismic performance of entire precast concrete frame structures explicitly incorporating realistic connection behavior remain relatively limited. Experimental studies on multi-story precast frames subjected to quasi-static cyclic loading demonstrated the significant influence of connection behavior on the global seismic response [33–35].

Several authors have addressed the numerical analysis of entire precast reinforced concrete (PRC) structures to investigate their seismic behavior. Comparative studies between precast and monolithic RC frames, and parametric analyses focusing on different modeling assumptions for precast systems, have been reported [36,37]. Numerical investigations of industrial single-story PRC buildings considering variations in structural configuration and seismic hazard levels have also been performed according to the current design codes [38]. Industrial precast reinforced concrete (PRC) buildings have specific characteristics that require careful consideration in seismic assessment. Several studies evaluated the influence of different modeling assumptions, including beam-to-column connections, roof-to-beam connections, system mass, and cladding, on both local and global seismic response [39–41]. One important conclusion from Fischinger et al. [21] highlights that minor differences in connection details can significantly alter structural behavior, and that experimental verification and inelastic analyses are essential for large-series prefabricated buildings in seismically active zones.

Existing PRC industrial buildings, especially those constructed before modern seismic design knowledge, have been the subject of a few vulnerability studies. Bosio et al. [42,43] investigated single-story PRC buildings in Italy to assess probabilistic seismic vulnerability and the effect of modeling choices on risk and retrofit requirements. Similarly, Batalha et al. [44] analyzed six Portuguese PRC buildings with common beam-to-column connections (pure friction and mechanical dowels), evaluating both local and global response under nonlinear static and dynamic analyses.

The main research objective of this study is to show how the outcomes from full-scale experiments of connections affect the structural analysis results and design procedures. The importance of experimental data for the creation of a reliable numerical model for dynamic analysis of a system with semi-rigid connections, such as PRC industrial halls, is pointed out. The description and results of the quasi-static full-scale experiments carried out up to failure on the models of four characteristic connections of the existing industrial building are presented. These results confirm the necessity of considering the nonlinear behavior and stiffness of connections in precast frame structures when determining displacements, which is particularly important for the verification of the serviceability limit state of structures in seismic regions. The simplified approach for taking into account stiffness reduction due to nonlinear behavior of element connections is proposed in the paper and applied for seismic

behavior assessment of the case study structure. This approach is also applicable for seismic risk assessment of existing industrial halls and commercial buildings constructed in the considered structural system, and for other PCR systems which are produced industrially in large series and which are designed for seismically active regions.

## 2. Case Study

The prototype of the hall (Figure 1) for the purpose of the numerical research was constructed according to the AMONT System (Morava Krušce) in Niš, Serbia. It was chosen considering that full-size tests of its connections had been previously conducted [45,46], but the recorded integral original results have not been presented or published in detail to date. Using unique, full-scale experimental test results, even if conducted nearly 30 years ago, is highly valuable today because of its direct applicability. Since the structural system has not changed, these results represent the "true" behavior of the current building stock in the Balkans, Italy, and Turkey. The results obtained from the conducted extensive experimental full-scale testing of the selected characteristic structural joints are highly important for advanced nonlinear modeling of this specific PRC system. Accurate modeling based on original tests allows engineers to design targeted retrofitting solutions where the original joints are most vulnerable.

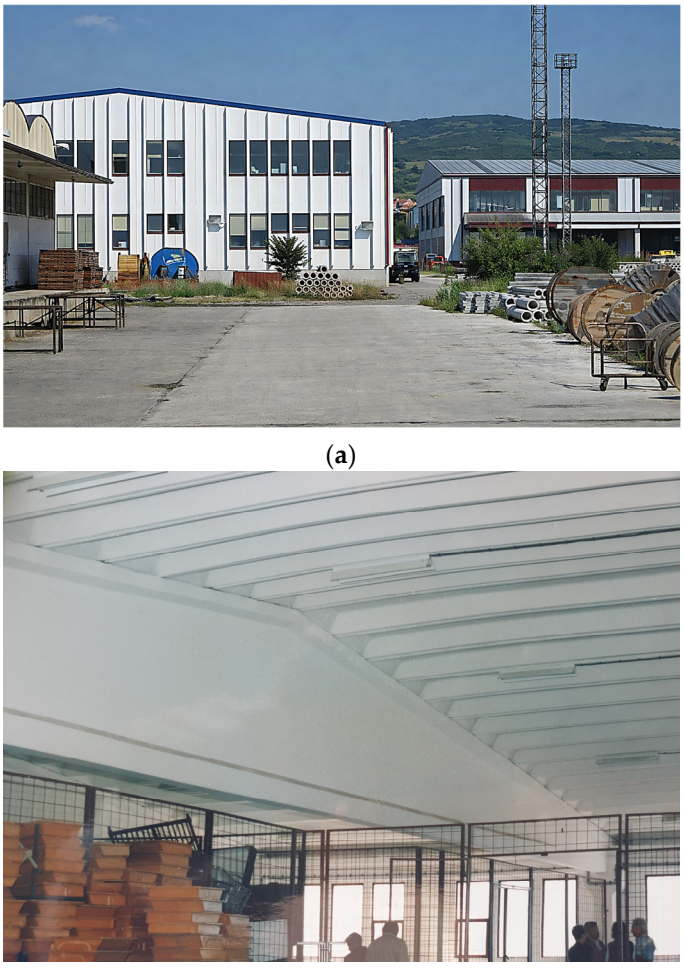

(**a**)

(**b**)

**Figure 1.** Existing industrial hall "Elektrotehna" in Nis, Serbia: (**a**) south façade; (**b**) interior on the first floor.

The existing hall is a spacious two-storey frame structure, and it is intended for storage of electrical materials and home appliances. The building was designed according to the

previous Serbian (former Yugoslav) code for the VIII seismic zone according to the MCS scale, which can approximately correspond to the peak acceleration of PGA = 0.20 g, but no direct dynamic analyses were performed. Only standard static analyses of the action of defined seismic forces for the transverse and longitudinal directions of the structure were performed. Therefore, this building was a suitable prototype for the realization of specific research for various seismic actions. In this way, and especially since the full-size tests of its connections were performed on the basis of which the results applied in this analysis were obtained, it was possible to give a much more accurate assessment of the structural system behavior and draw relevant conclusions about the degree of seismic resistance of the system in the zones of different seismic intensity.

The facility was built in 1986. An on-site inspection of the building revealed that the building exhibited no noticeable structural or non-structural damage. The general conclusion was that the behavior of the facility during the previous service period was satisfactory. This indicates the fact that the quality of the installed materials and the quality of the prefabricated elements as a whole are at a satisfactory level.

### *2.1. Structure Description*

The basic structural system of the building, whose layout and cross-sections are shown in Figure 2, consists of the prefabricated structural elements shown in Figure 3. The real joints of the prototype hall, constructed according to the AMONT System, are represented in Figure 4.

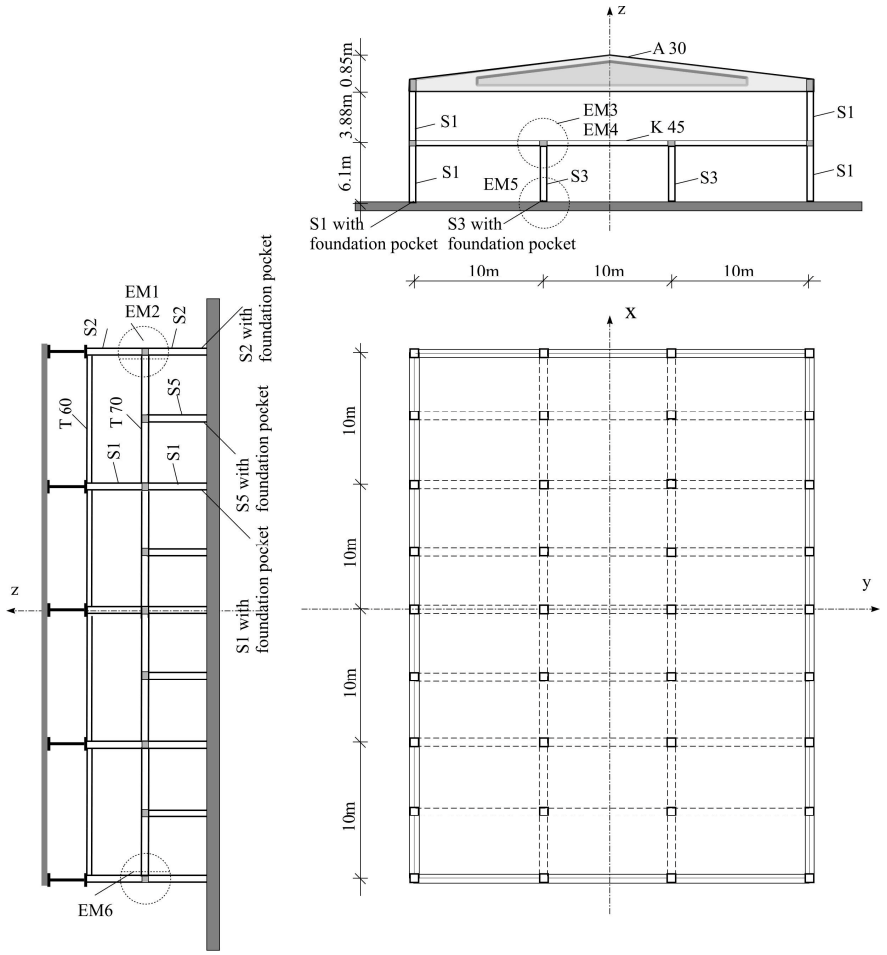


**Figure 2.** Ground floor layout, longitudinal and transverse section of the industrial hall (tested connections are marked and designated as EM-1–EM-6).

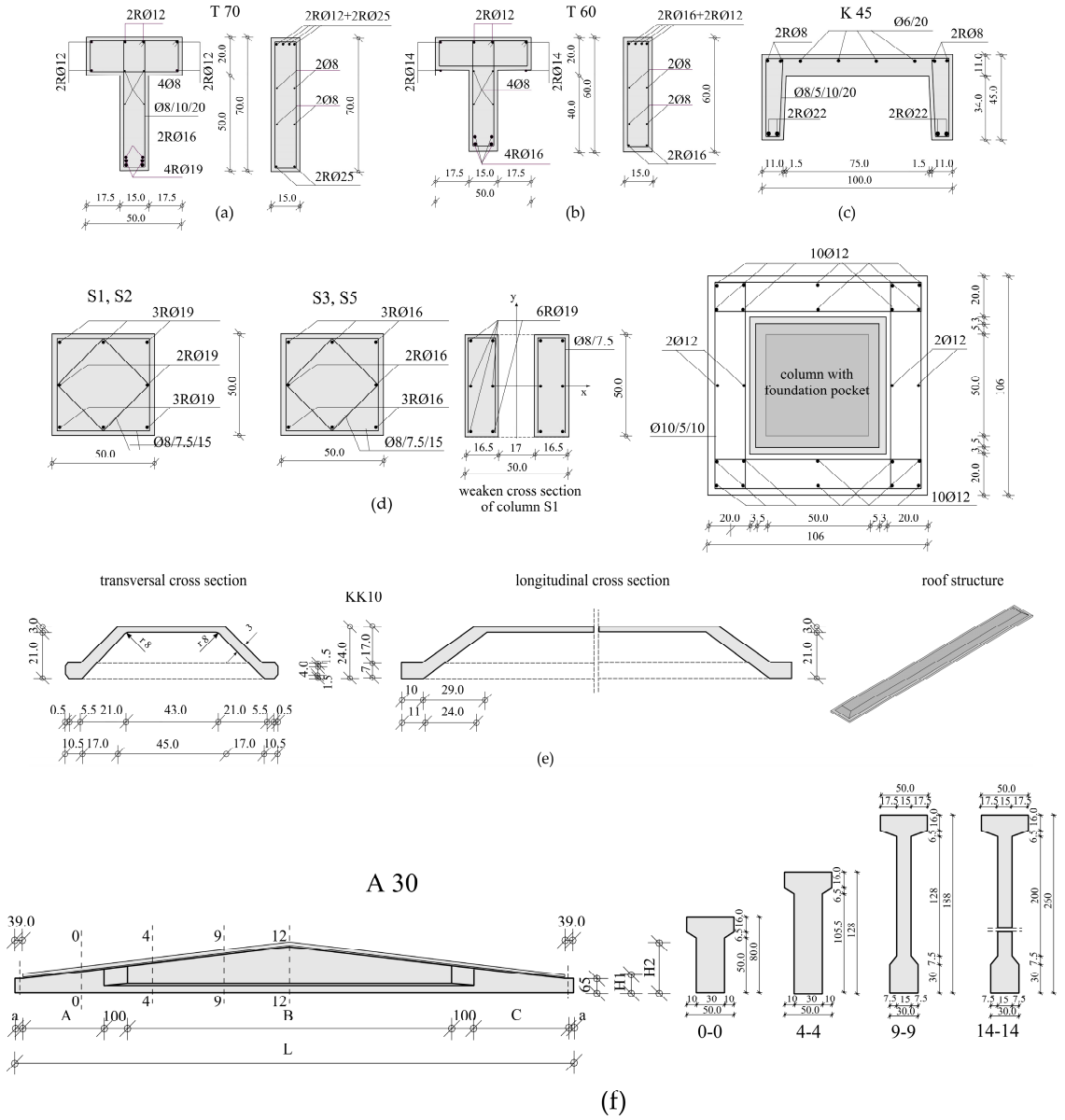


**Figure 3.** The elements of the considered precast industrial hall: (**a**,**b**) floor beams, (**c**) element of floor structure K 45, (**d**) columns and column with foundation pocket, (**e**) element of roof structure, (**f**) roof beam (main girder).

(**a**) (**b**) (**c**) (**d**)

**Figure 4.** Connections of the existing industrial hall "Elektrotehna" in Nis, Serbia: (**a**) corner column—main roof girder; (**b**) mid column—main roof girder; (**c**) corner column—floor girder; (**d**) interior column—floor girder above the ground floor.

The structure consists of precast columns, floor beams, floor structure, and roof beams.

The main roof beams carry the roof elements. They are designed as beams of variable height, with a two-sided slope of the upper edge of about 12°, designated as A-30

(Figures 2 and 3f). The main roof beams are made of concrete class C40 (C40 stands for the 40 MPa concrete compressive strength obtained experimentally on the cube specimens with an edge size of 200 mm). The main roof girders A-30 are adhesively pre-stressed with a span of 30.0 m, with an I-shaped cross-section at the point of support, which gradually forms into a T-shaped cross-section with a height of 80 cm, while in the middle of the span, its height is 260 cm. In addition to the reinforcement cables, 7 rows of 7 cables 7ϕ3 arranged in the lower zone of the beam, it is also reinforced by the non-structural reinforcement 6 Rϕ16 at the beam flange, 4 Rϕ16 at the bottom flange of the beam, and 22 Rϕ16 in the beam web. Secondary girders on the roof level (connecting girders) extend in the longitudinal direction of the building. They are designed as T-60 (designation stands for "T" cross-section and cross-section height) of constant height and span of 10.0 m (Figures 2 and 3b), and made of concrete class C30.

The floor structure is made of trapezoidal elements designated as K45 (Figures 2 and 3c), made of C40 concrete.

The main girders of the floor carry the floor slabs. These girders extend in the longitudinal direction of the object. They are of constant height, span 5 m, and are designed as T-90 in the central part and as T-70 (Figures 2 and 3a) around the perimeter of the structure. The secondary girders of the floor extend in the transverse direction only around the perimeter of the building and are designed as T-40, constant height, and span of 10.0 m. The floor girders are made of concrete class C30.

All columns are prefabricated, square cross-section 50/50 cm, fixed in foundation pockets, and made of concrete class C30.

The building is entirely founded on the foundation footings. The peripheral parapet walls were constructed on the foundation beams designed for this purpose. The building is on the façade, enclosed by prefabricated façade corrugated elements.

Connection of precast elements is completed by anchors, welding, and grouting with small-sized aggregate concrete. This procedure is known as the wet procedure.

### *2.2. Quasi-Static Tests of the Full-Scale Models of Connections up to Failure*

Experimental laboratory investigation of bearing capacity and deformability of chosen connections was conducted at the Institute for Earthquake Engineering and Engineering Seismology (IZIIS) in Skopje, Macedonia [45]. The essential aim of this investigation was attesting of static and dynamic stability of the most significant and typical modulus of a hall program of the considered precast RC structural system AMONT, developed in company Morava Krušce, Serbia.

In the case of the presented research, optimization of the experimental program was made so that models of the characteristic structural fragments were tested, instead of testing all structural elements and their connections, upon which it was possible to draw very useful conclusions about the integral system behavior. The results of these tests were used in numerical analysis, which is the focus of this paper.

#### 2.2.1. Procedure of Quasi-Static Tests

All models were internally instrumented and constructed in the company's facilities in Krušce, Serbia, and transported to the Institute (IZIIS) in Skopje to the laboratory for dynamic tests. The elements and joints were designed according to the project documentation of the existing building.

One or two horizontal pistons (servo actuators) with a capability of a maximum input force of 1500 kN or 1000 kN were used for loading input, depending on the experimental model. Displacement measuring instruments (LVDTs) with different ranges were placed at characteristic points, marked on experimental models in advance. The force that is applied

in servo actuators and displacement of the piston were measured during the tests. It is worth mentioning that lateral displacement in quasi-static tests was applied in a series of three cycles with the same maximum amplitude, with the maximum amplitude in each series being greater than that of the previous one, which is in accordance with the widely adopted testing procedure. The lateral displacement amplitude was increased until a significant nonlinear response of the connections was observed.

The whole process of programmed cyclic displacement was controlled and conducted by use of a linear potentiometer. Data processing was carried out by specific software. Data processing and analysis enable review of the hysteresis nonlinear relation force-deformation, hysteresis nonlinear relation moment–rotation for characteristic cross-sections, stiffness degradation, propagation and spreading of cracks, and capacity of connection ductility in conditions of cyclic loading up to failure, which is particularly significant to prove the reliability of the system in seismic regions.

#### 2.2.2. Corner Column to Girder of Floor Structure Connection

Experimental examination of the characteristics of the nonlinear behavior of the connection of the floor beam to the corner column was performed on two full-size physical models designated as experimental model-1 (EM-1) and experimental model-2 (EM-2), as shown in Figure 5. These two identical models, among other things, make it possible to determine the actual level of potential variation in the quality of construction of a prefabricated semi-rigid connection. Part of the prefabricated column, 50 × 50 cm, is supported by two metal brackets and fastened with bolts that ensure complete restraint. In two existing orthogonal openings, two floor beams were fitted: one short (for simulation) and one long. The goal of the experiment was to determine the effective degree of restraint of the longer T-70 standard beam, which has a tenon inserted into the opening of the corner column. This connection was joined by the standard procedure of grouting using cement mortar implemented by the contractor. The testing of the T-70 beam restraint degree was performed under the simultaneous action of constant axial force and cyclic transversal force guided along the cyclic displacement record with various amplitudes to failure. The level of axial force was defined, and the way and sequence of applied transversal cyclic displacements are shown in Figures 6 and 7. Initially an axial force of N = 75 kN was applied by a stronger servo actuator with the purpose of compensating for the effect of the gravity load lateral to the considered connection. Subsequently, cyclic displacements were applied using a smaller servo actuator. The amplitude of displacement at the end of the beam T-70 was successively monotonously increased by this actuator, up to failure of the connection. Displacement was applied in a series of three full cycles with the same maximum amplitude, while the maximum amplitude was increased in each subsequent series.

In this way, the force intensity for each displacement value was registered, and the hysteresis force–displacement dependence was obtained. The applied instrumentation for the critical transverse direction enabled the registration of rotations at each amount of force. Thus, using the known force, the value of the bending moment was obtained, and so the (M-ϕ) real hysteresis dependences of the moment-curves were generated, which have a great importance in the formulation of the model for simulation of the real behavior of semi-rigid connections. The form of these dependences is very similar to the obtained hysteresis force–displacement dependences.

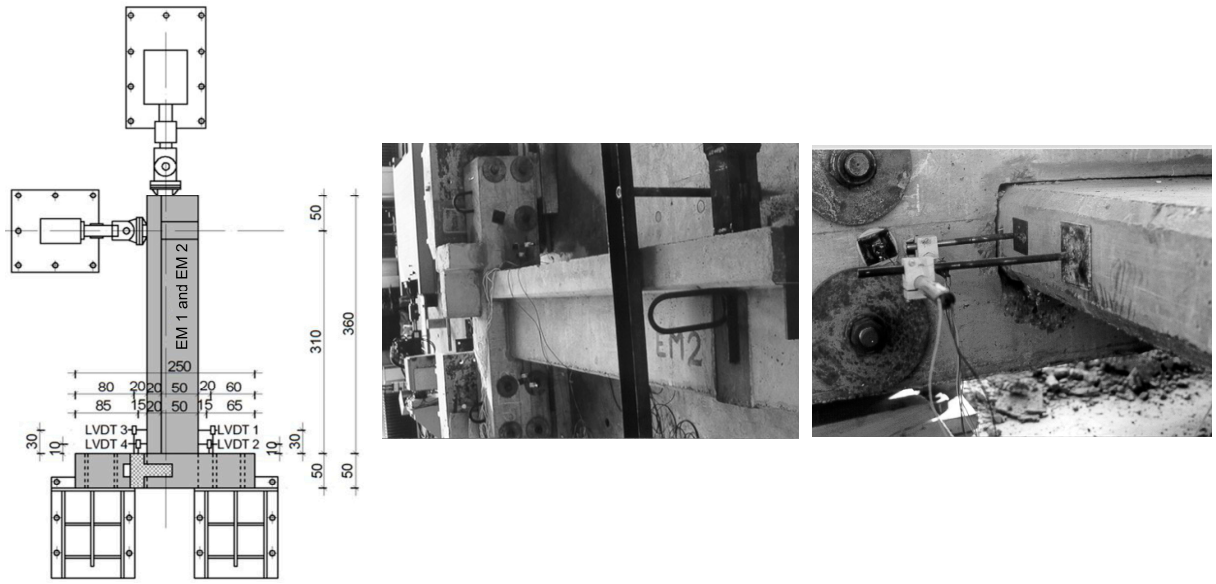


(**a**) (**b**) (**c**)

**Figure 5.** Connection corner column to floor beam: (**a**) cross-section of the models EM-1 and EM-2; (**b**) setup of the model EM-2; (**c**) failure of the model EM-2 [45].

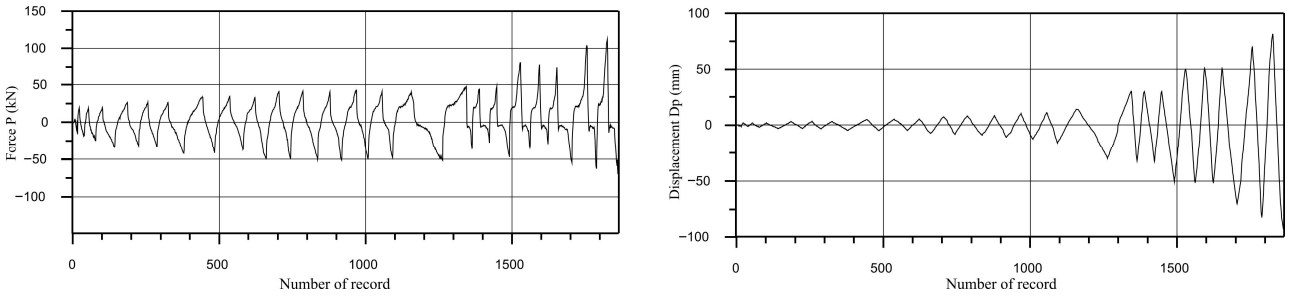


(**a**) (**b**)

**Figure 6.** EM-1: (**a**) history of lateral cyclic force at the end of the beam; (**b**) history of displacement of the end of the beam in the lateral direction [45].

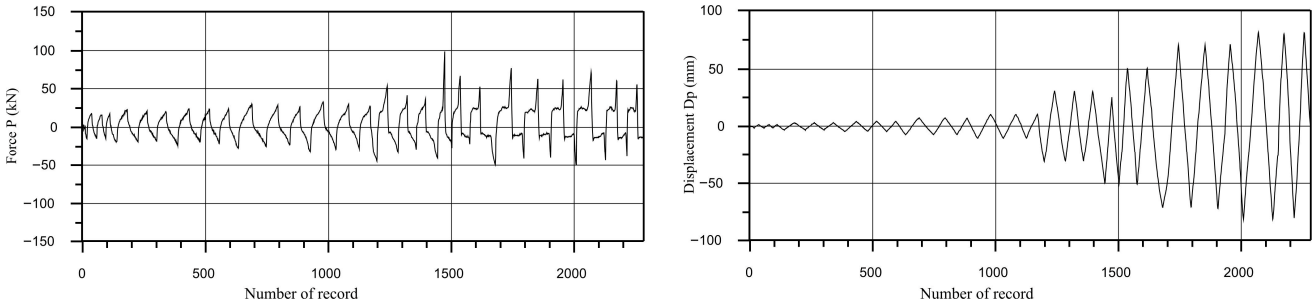


(**a**) (**b**)

**Figure 7.** EM-2: (**a**) history of lateral cyclic force at the beam end; (**b**) history of displacement of the beam end in the lateral direction [45].

Cyclic force P-displacement diagram of the end of the beam and moment–rotation diagram of the connection column to beam for models EM1 and EM2 are shown in Figures 8 and 9, respectively.

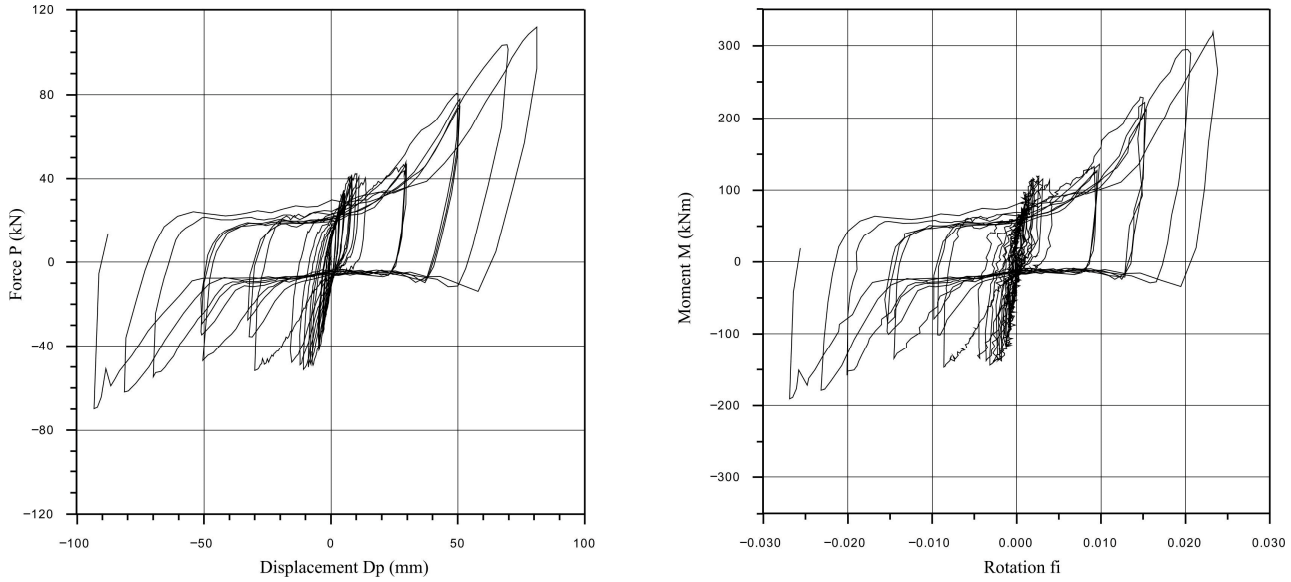


(**a**) (**b**)

**Figure 8.** EM-1: (**a**) relation cyclic force–displacement of the beam end; (**b**) relation moment–rotation (base LVDT-1 and LVDT-3) [45].

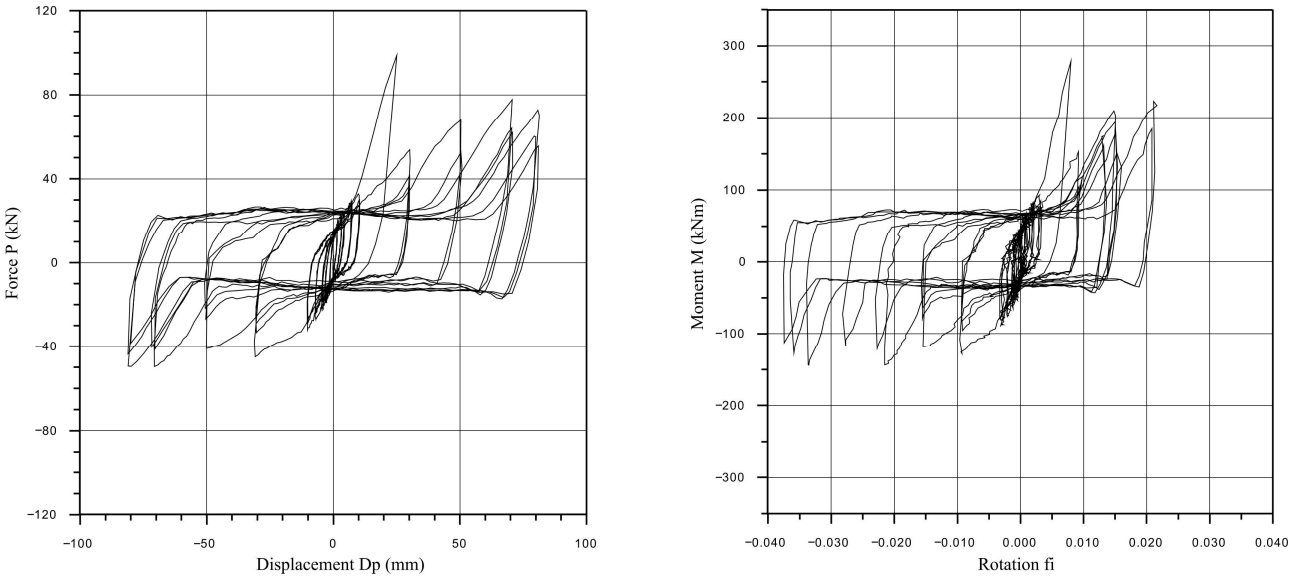


(**a**) (**b**)

**Figure 9.** EM-2: (**a**) relation cyclic force–displacement of the beam end; (**b**) relation moment–rotation (base LVDT-1 and LVDT-3) [45].

### 2.2.3. Floor Structure to Floor Beam Connection

Providing of data about bearing capacity and deformability of the connection of floor structure elements K-45 with the floor beam, i.e., about transmission of negative moments at the point of support above the floor beam T-70, was carried out using almost two identical models, EM-3 and EM-4, as shown in Figure 10. The difference between these two models is in the amount of montage reinforcement placed in the continuity layer. In the model EM-3, only one reinforcement mesh, Q-131, and in the model EM-4, two such meshes were embedded. In addition, the side contact of the head of beam T-70 was grouted with ribs of floor elements K-45 in the model EM-4. The level of rigidity of this connection was observed when the construction was finished.

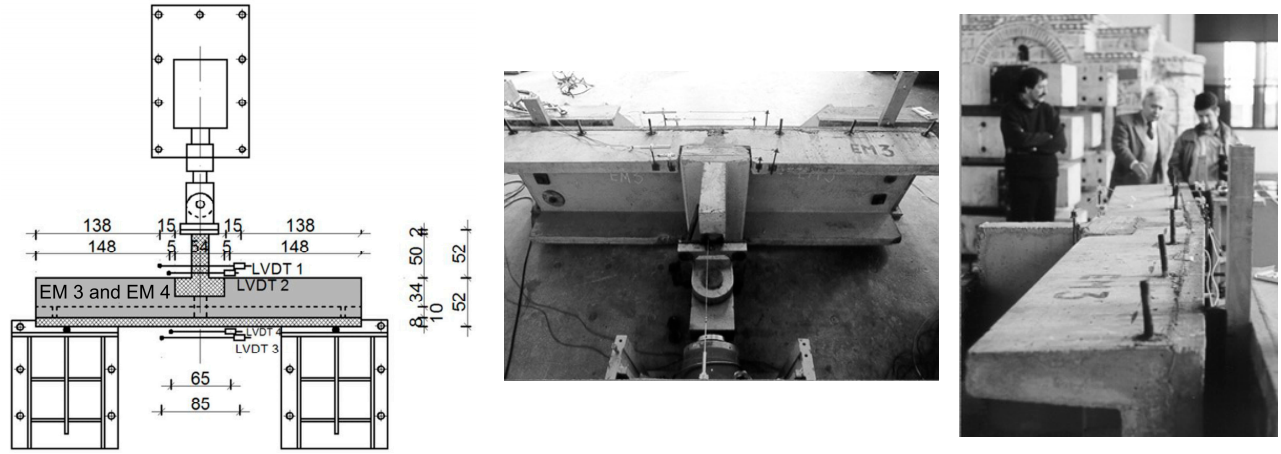


(**a**) (**b**) (**c**)

**Figure 10.** Connection floor structure to floor beam: (**a**) cross-section of the models EM-3 and EM-4; (**b**) setup of the model EM-3; (**c**) large deformations of the model EM-3 at the point of support [45].

Composition of the EM-3 and EM-4 models of the connection floor element to the floor beam was tested up to failure as well. Cyclic displacement of the rib of the beam (Figures 11 and 12) simulated the influence of negative moment with gradually increasing intensity at the support of two floor elements from neighboring bays.

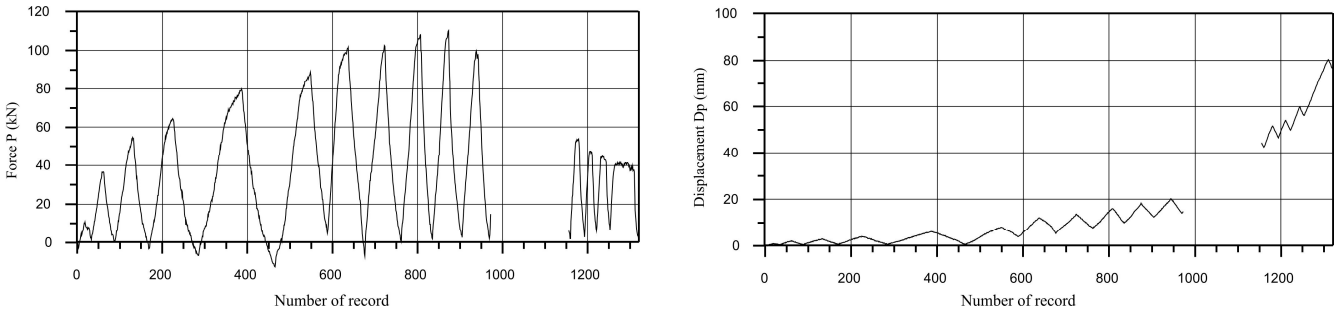


(**a**) (**b**)

**Figure 11.** EM-3: (**a**) history of cyclic force applied to the rib of the beam, (**b**) history of displacement of the rib of the beam [45].

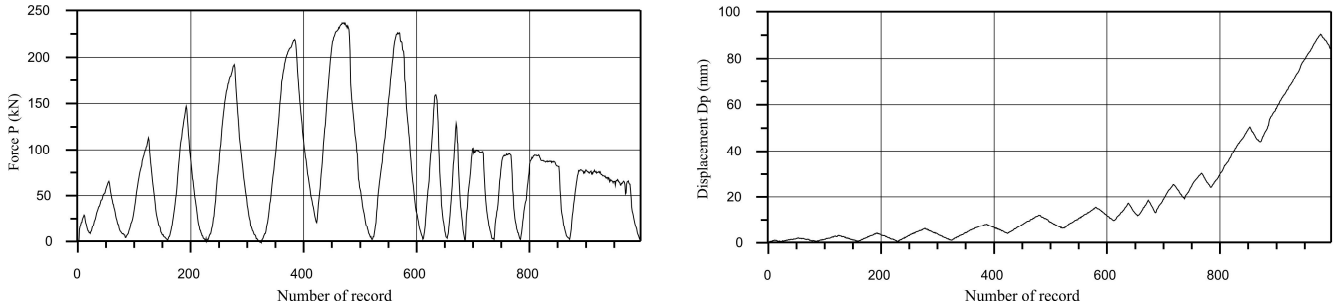


(**a**) (**b**)

**Figure 12.** EM-4: (**a**) history of cyclic force applied to the rib of the girder; (**b**) history of displacement of the rib of the beam [45].

Cyclic force P-displacement diagram of the rib of the girder T-70 and moment–rotation diagram of the floor element K-45 at the support on the beam T-70 (models EM-3 and EM-4) are shown in Figures 13 and 14, respectively.

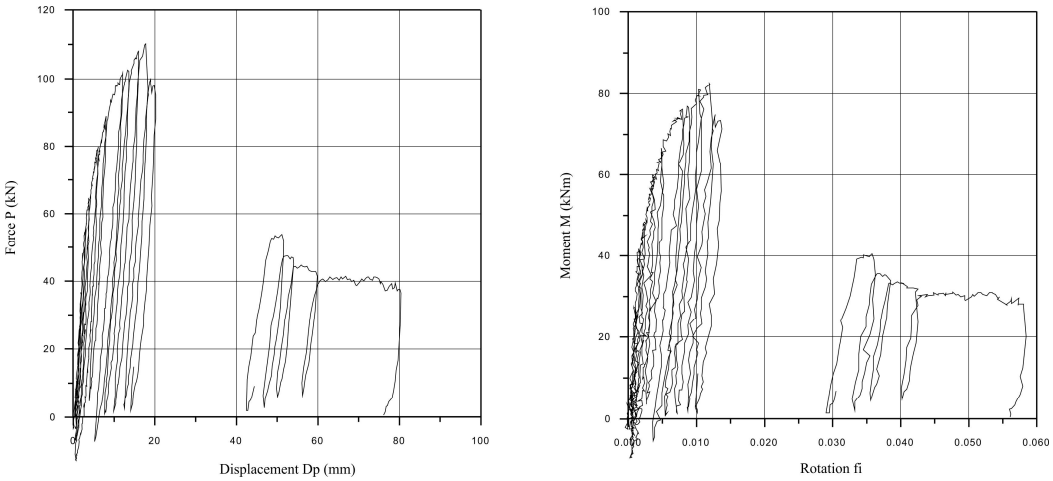


**Figure 13.** EM-3: (**a**) relation cyclic force–displacement of the rib of the beam T-70; (**b**) relation moment–rotation of the floor element K-45 at the support on the beam T-70 (base LVDT-1 and LVDT-3) [45].

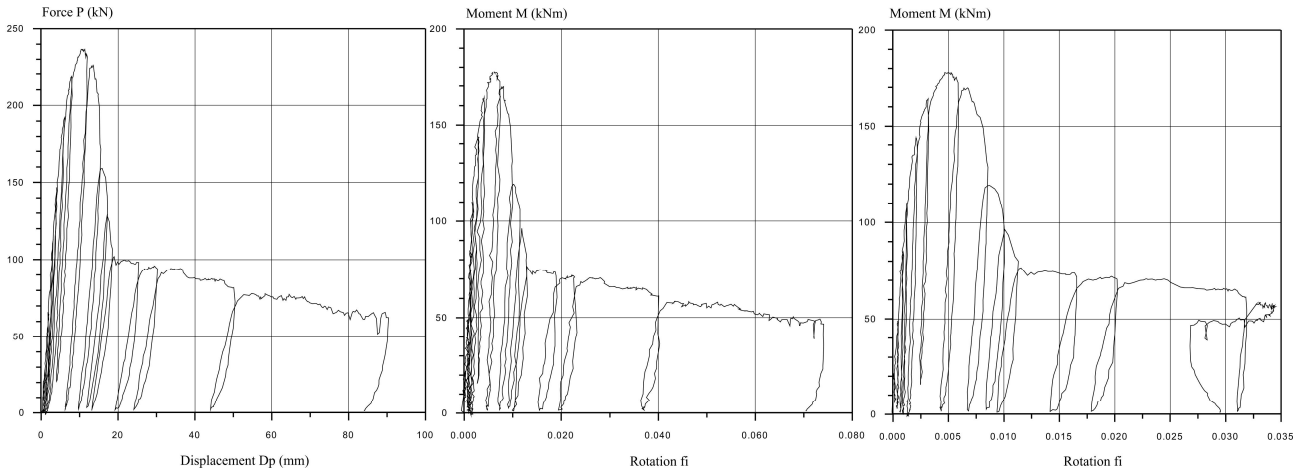


**Figure 14.** EM-4: Relation (**a**) relation cyclic force–displacement of the rib of beam T-70; (**b**) Relation moment–rotation (base LVDT-2 and LVDT-4); (**c**) relation moment–rotation (base LVDT-1 and LVDT-3) [45].

### 2.2.4. Column to Foundation Connection

The connection of a precast RC column 50/50 cm to the foundation pocket was investigated using the model EM-5, as shown in Figure 15. Static vertical axial force and transverse increasing cyclic force up to failure were applied as loading.

Testing of the model EM-5 was performed so that at first the axial force N = 385 kN was applied by stronger servo actuator with the purpose of simulating an expected gravity load in the considered cross-section of the column during exploitation, and then displacement amplitude of the column end was increased successively monotonously using smaller servo actuator, up to nonlinear behavior of the connection and the column, as shown in Figure 16.

Cyclic force–displacement diagram of the column end and moment–rotation diagram of the column at its connection to the foundation pocket are shown in Figure 17. It can be concluded that this type of connection shows stable hysteretic behavior up to failure. There is no significant degradation during the repeated loading cycles with the same amplitude, but the connection stiffness degradation occurs at higher load levels due to the

concrete cracking and crushing (especially of the concrete cover). The hysteresis shows satisfying ductile behavior of the connection (energy dissipation), with a clear pinching effect characteristic of the RC joints.

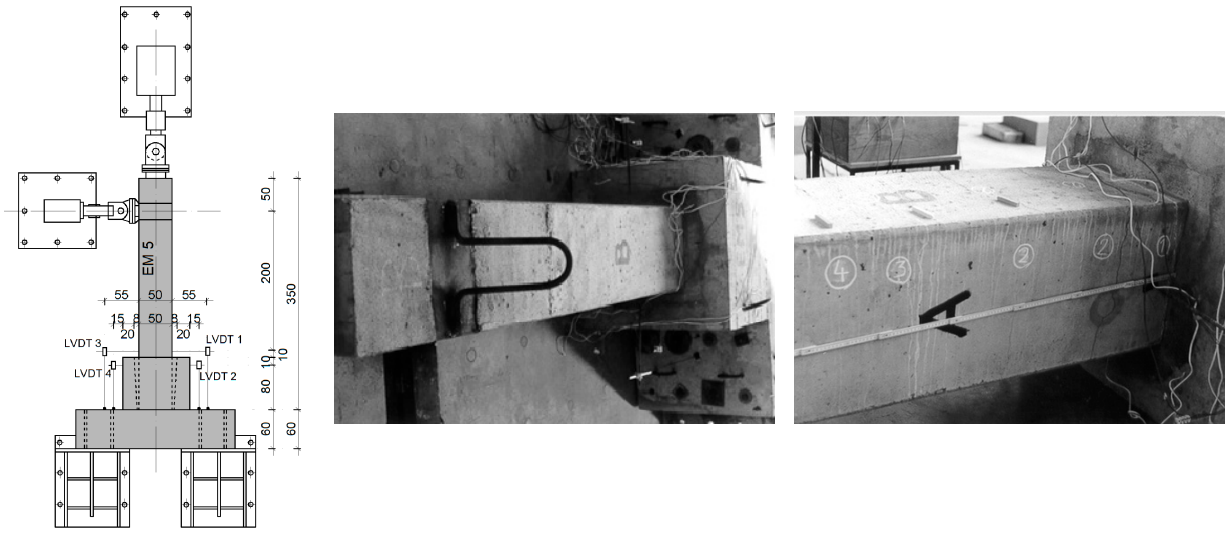


(**a**) (**b**) (**c**)

**Figure 15.** Connection column to foundation: (**a**) cross-section of the model EM-5; (**b**) setup of the model EM-5; (**c**) crack propagation in the model EM-5 [45].

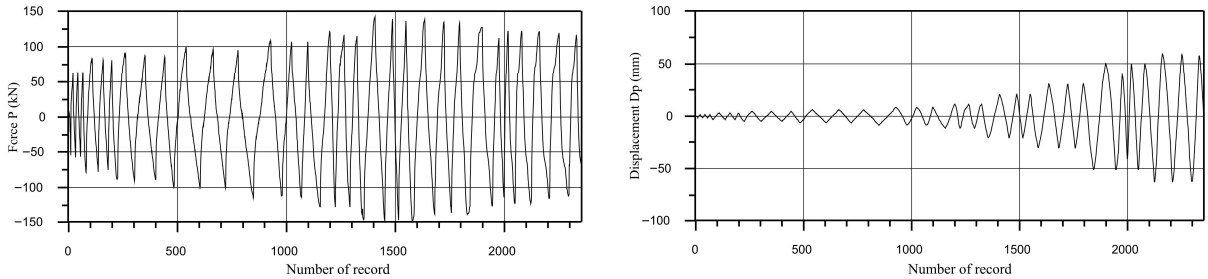


(**a**) (**b**)

**Figure 16.** EM-5: (**a**) history of lateral cyclic force at the column end; (**b**) history of displacement of the column end in the lateral direction [45].

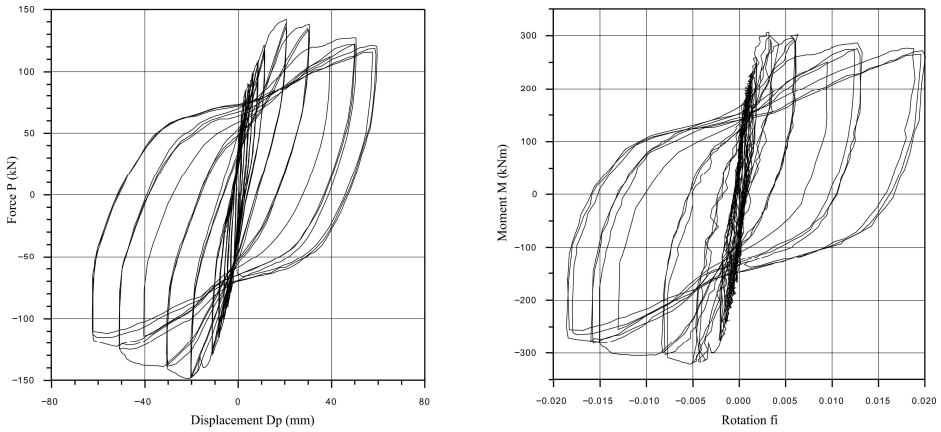


(**a**) (**b**)

**Figure 17.** EM-5: (**a**) relation cyclic force–displacement of the column end; (**b**) relation moment–rotation (base LVDT-1 and LVDT-3) [45].

2.2.5. Corner Column to Beam Connection

Test of the model EM-6 was performed to find out data about bearing capacity and deformations of the weakened column at the connection point with the floor beam, as shown in Figure 18, up to failure. Loading was a vertical static axial force at the second-story level and an increasing lateral cyclic force up to failure of the connection.


(**a**) (**b**) (**c**)

**Figure 18.** Disposition of experimental model EM-6 of the connection of the floor beam to weakened corner column: (**a**) cross-section of the model EM-6; (**b**) setup of the model EM-6; (**c**) crack propagation in the model EM-6 [45].

Testing of the model EM-6 was performed according to the prepared loading program. The axial force N = 285 kN was applied at first by a stronger servo actuator with the purpose of simulating an expected gravity load in the considered cross-section of the column during exploitation. Then displacement amplitude of the column end was increased successively monotonously using a smaller servo actuator, up to deeply nonlinear behavior of the connection and the column, as shown in Figure 19.

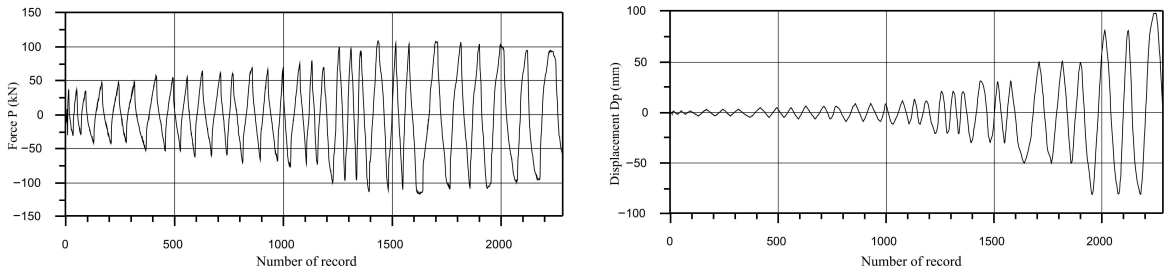


(**a**) (**b**)

**Figure 19.** EM-6: (**a**) history of lateral cyclic force at the column end; (**b**) history of displacement of the column end in the lateral direction [45].

Cyclic force–displacement diagram of the column end and moment–rotation diagram of the column at its connection with the floor girder are shown in Figure 20. Similarly to the connection EM5, this connection has stable hysteretic and ductile behavior up to failure, with the stiffness degradation at higher load levels and pinching of hysteresis. It can be concluded that the weakened column at the connection point with the floor beam provides adequate nonlinear behavior for the application in the seismic-prone regions.

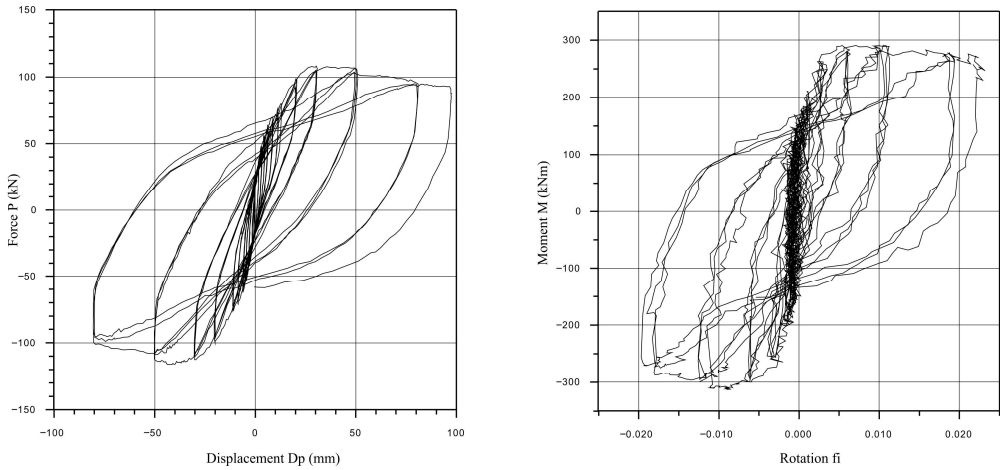


(**a**) (**b**)

**Figure 20.** EM-6: (**a**) relation cyclic force–displacement of the column end; (**b**) relation moment–rotation (base LVDT-1 and LVDT-3) [45].

### 2.2.6. Frame Beam to the Column Connection

For the direct dynamic analysis of the considered industrial precast structure, it is necessary to define the moment–rotation relationship for the connection of the frame beam T70 with the column. The experimental testing of this connection has not been conducted. Therefore, the theoretical moment–rotation diagram, as shown in Figure 21, is defined using the dedicated computer program SECAP (Section Capacity) developed at IZIIS. The calculation is based on the fiber model, in which the section is discretized into a finite number of fibers. Each fiber is represented by a stress–strain relationship based on the material characteristics in its tributary area. Based on the plane sections assumption (Bernoulli hypothesis), and the equilibrium of section forces, the moment–rotation relationship of the section is defined through the characteristic discrete points. Considering that the flange of the beam is cut off at the connection, the geometric characteristics and reinforcement of the cross-section's rib are used in the theoretical analysis, along with material characteristics of the concrete class C30, compressive strength on cubic specimen 30 MPa and modulus of elasticity 31.5 GPa, and reinforcement yield stress of 400 MPa and modulus of elasticity 210 GPa.

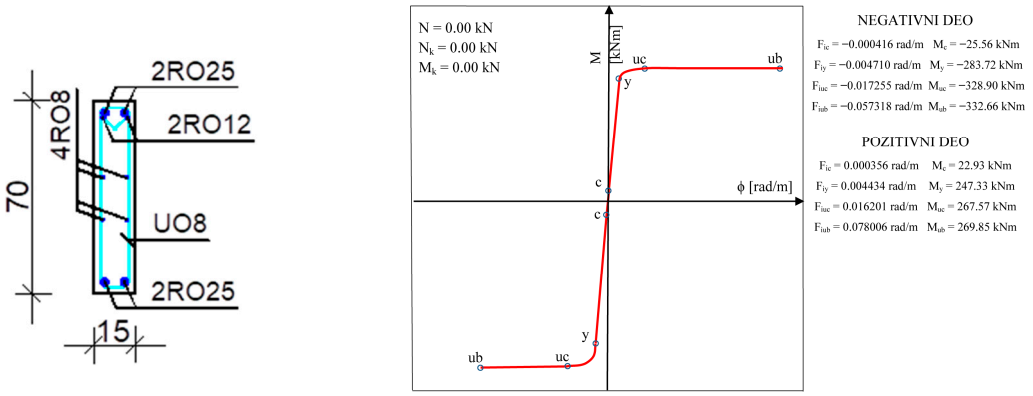


(**a**) (**b**)

**Figure 21.** T-70 connection to column: (**a**) geometry and reinforcement; (**b**) relation moment–rotation.

## 3. Modeling of the Structure and Numerical Analysis

The seismic response of a structure can be obtained based on the nonlinear direct dynamic analysis, introducing the experimentally and theoretically obtained moment–rotation (M-ϕ) relationships of precast concrete frame connections. On the other hand, the implementation of nonlinear dynamic analysis in everyday engineering practice can be demanding [47,48]. Therefore, the aim is to propose a simplified model of the structure in order to calculate the roof top displacement considering the effects of the connections' stiffness.

The proposed simplified approach, applicable in engineering practice, consists of two steps: The first step involves materially linear and geometrically nonlinear dynamic analysis in order to obtain bending moments in the vicinity of the frame connections. Further, the obtained bending moments using materially linear analyses are combined with the experimentally/theoretically defined moment–rotation relationships to calculate stiffness change in the connections. This proposed approach is schematically presented in Figure 22. The second step involves materially linear and geometrically nonlinear dynamic analysis with defined stiffness of the connections according to the previous step. The main goal is to obtain displacements of the structure using materially linear analysis instead of nonlinear direct time history analysis. Although standard provisions [49–52] require that possible response degradation of connections should be taken into account, there are no, or at least, there are limited instructions for the determination of connection stiffness and resistance. Therefore, this proposed approach represents an attempt to provide a simplified but valid model that considers connection stiffnesses based on experimental and/or theoretical moment–rotation relationships, making it practical for everyday engineering.

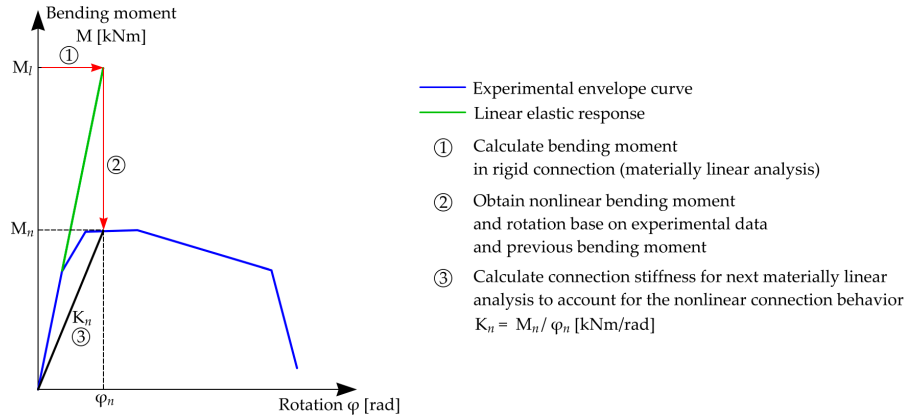


**Figure 22.** Schematic definition of nonlinear connection stiffness based on the materially linear analysis of a frame with rigid connections and experimental nonlinear response of the connection.

The described procedure was conducted on a model consisting of two orthogonal planar frames, since the structure considered in this study meets the requirements prescribed for such an approach in EC8 [49], under the action of two real earthquake records with characteristic frequency–amplitude content. The following seismic excitations (ground-acceleration time history records) were selected, as shown in Figure 23: (1) Montenegro earthquake of 15 April, 1979 (N–S component), Ulcinj–Albatros station; (2) El Centro earthquake of May 18, 1940 (S00E component). Namely, El Centro is adopted worldwide as a benchmark in nonlinear seismic analysis, while Ulcinj–Albatros accelerogram represents a significant earthquake record for the Balkan region, where the considered precast structure is used. Therefore, these two earthquake records are adopted in the analysis. Considering that the significant nonlinear deformations do not occur at lower levels of ground acceleration, the analyses are performed by scaling the records to the level of maximum peak ground acceleration of 0.4 g (g stands for the gravitational acceleration g = 9.81 m/s$^2$).

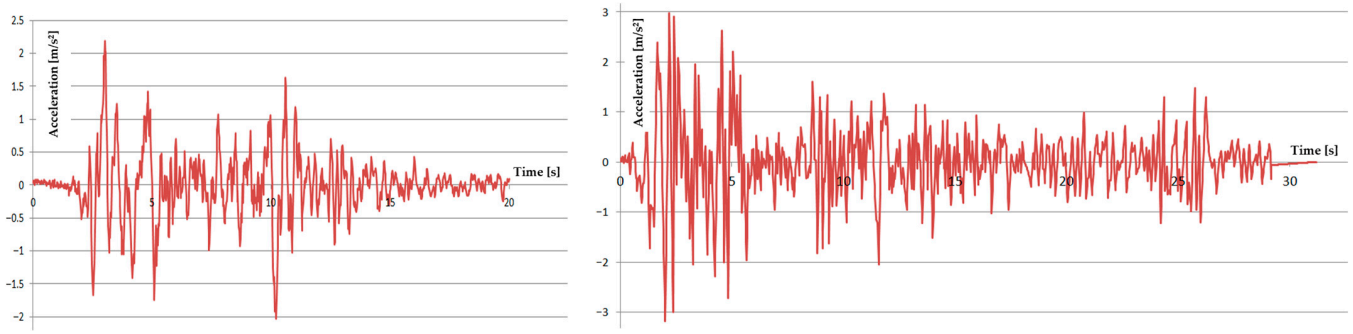


**Figure 23.** Earthquake accelerograms (unscaled): (**a**) Ulcinj–Albatros (N–S component); (**b**) El Centro (S00E component).

The finite element analysis was performed using the software ETABS 22, suitable for dynamic analysis using direct integration of equations of motion in the time domain, including material and geometric nonlinearities [53]. The geometry of the model was evaluated in accordance with the geometry of the building (Figures 2 and 3), where the models of the transverse and longitudinal frames are presented in Figure 24. The columns and beams were modeled by 1D beam finite elements (FE). The mesh sensitivity analysis was performed for both frames for different FE lengths: 0.25 m, 0.50 m, and 1.00 m. Considering that the roof top displacements are almost identical for different mesh sizes, the FE length of 0.5 m was adopted. Concrete is modeled as an isotropic linear elastic material, whereby the Poisson's ratio is 0.20 and modulus of elasticity is 31.5 GPa and 34 GPa for concrete classes C30 and C40, respectively. At the foundation level, appropriate fixed supports are defined in the model.

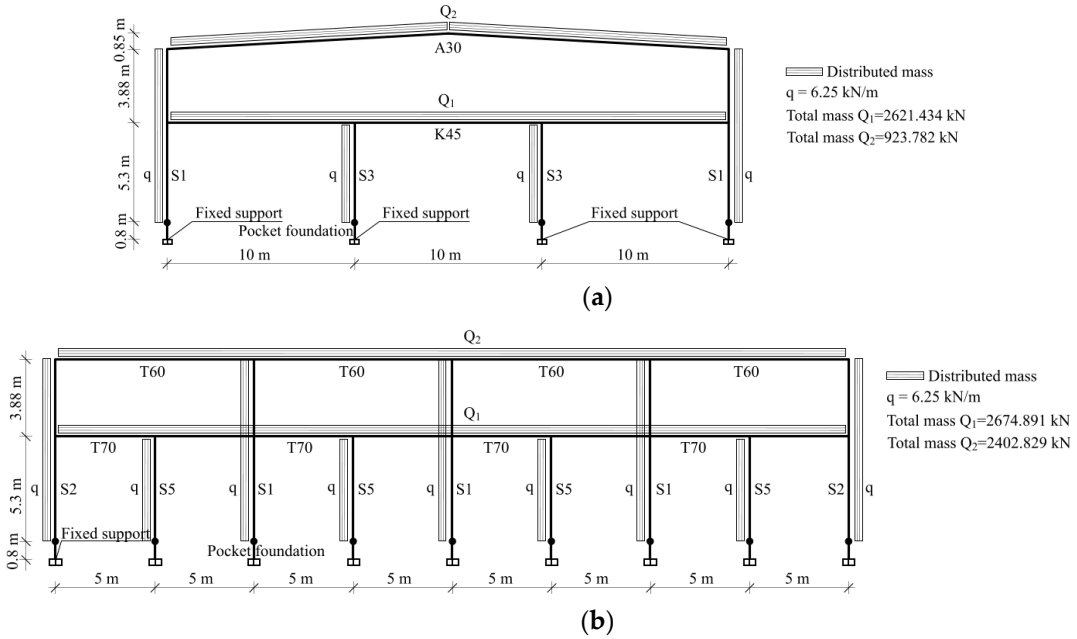


**Figure 24.** Finite element model for linear direct dynamic analysis: (**a**) transverse frame; (**b**) longitudinal frame.

The geometric nonlinearity was included using P-Δ and the large displacement method built into the software (equilibrium equations are formulated in the deformed configuration of the structure at each load step). Nonlinear dynamic analysis was conducted with a time increment of 0.01 s, which corresponded to the discrete values of applied accelerograms.

The calculation includes the damping of 5% defined by the Rayleigh model using vibration periods of the first two modes for each frame, as shown in Figure 25. The integration of the dynamic equations is performed by the implicit Hilber–Hughes–Taylor method, where the integration parameters are $\alpha = 0$, $\beta = 0.25$, and $\gamma = 0.5$ [53,54].

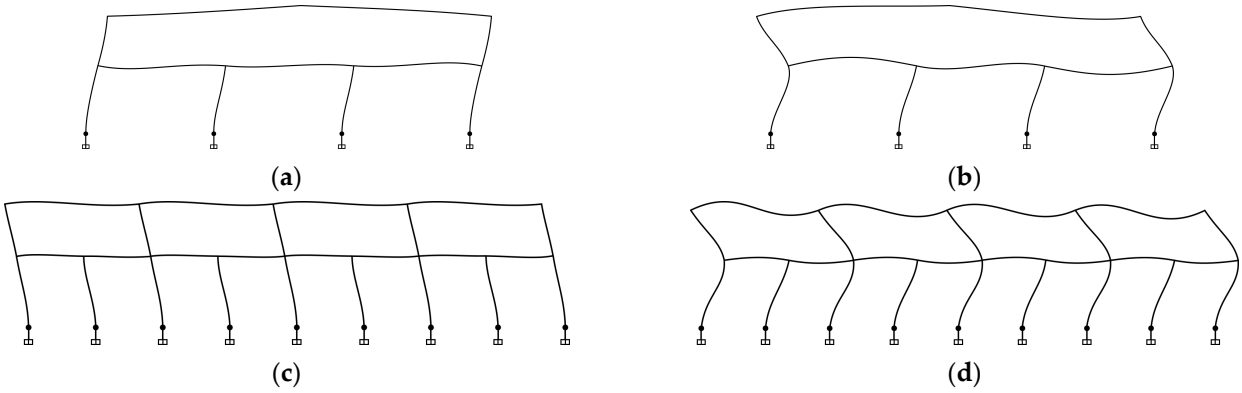


**Figure 25.** Mode shapes of analyzed frames: (**a**) transverse frame—I mode ($T_1 = 0.685$ s); (**b**) transverse frame—II mode ($T_2 = 0.218$ s); (**c**) longitudinal frame—I mode ($T_1 = 0.549$ s); (**d**) longitudinal frame—II mode ($T_2 = 0.191$ s).

Based on the bending moments in the different connection joints obtained from the materially linear dynamic analysis on the models with rigid joints, the connection's stiffness was calculated according to the proposed procedure (see Figure 22). Such calculated connection stiffnesses, shown in Tables 1 and 2, were used in the second model as frame elements end releases stiffness in order to obtain the roof top displacements and inter-story drift ratios at the time of maximum roof top displacement of the analyzed frames under the considered earthquake acceleration records (Tables 3 and 4).

**Table 1.** Stiffness of the analyzed connections for the transverse frame.

| Connection Type | Ulcinj–Albatros | | | |
|---|---|---|---|---|
| | $M_l$ [kNm] | $M_n$ [kNm] | $\varphi_n$ [rad] | $K_n$ [kNm/rad] |
| EM4 | 764.20 | 162.74 | 0.002732 | 59,568.08 |
| EM5 (end columns) | 1249.52 | 300.00 | 0.003250 | 92,307.69 |
| EM5 (middle columns) | 972.61 | 300.00 | 0.002530 | 118,577.10 |
| EM6 | 881.53 | 233.60 | 0.000626 | 373,282.20 |
| **Connection type** | **El Centro** | | | |
| | $M_l$ [kNm] | $M_n$ [kNm] | $\varphi_n$ [rad] | $K_n$ [kNm/rad] |
| EM4 | 864.37 | 167.31 | 0.003090 | 54,145.63 |
| EM5 (end columns) | 1489.64 | 300.00 | 0.003879 | 77,339.52 |
| EM5 (middle columns) | 1098.40 | 300.00 | 0.002857 | 105,005.30 |
| EM6 | 1020.24 | 243.49 | 0.000724 | 336,172.86 |

**Table 2.** Stiffness of the analyzed connections for the longitudinal frame.

| Connection Type | Ulcinj–Albatros | | | |
|---|---|---|---|---|
| | $M_l$ [kNm] | $M_n$ [kNm] | $\varphi_n$ [rad] | $K_n$ [kNm/rad] |
| EM4 (end connections) | 1164.64 | 130.12 | 0.002309 | 56,358.28 |
| EM4 (middle connections) | 934.20 | 116.07 | 0.001851 | 62,696.48 |
| EM5 (end columns) | 1046.71 | 300.00 | 0.002722 | 11,021.31 |
| EM5 (middle columns) | 1278.12 | 300.00 | 0.003324 | 9025.27 |
| EM6 | 671.13 | 306.93 | 0.011155 | 27,515.02 |
| **Connection type** | **El Centro** | | | |
| | $M_l$ [kNm] | $M_n$ [kNm] | $\varphi_n$ [rad] | $K_n$ [kNm/rad] |
| EM4 (end connections) | 1294.08 | 145.51 | 0.002566 | 56,711.36 |
| EM4 (middle connections) | 1033.05 | 122.10 | 0.002048 | 59,630.79 |
| EM5 (end columns) | 1232.91 | 300.00 | 0.003207 | 93,545.37 |
| EM5 (middle columns) | 1475.09 | 300.00 | 0.003837 | 78,186.08 |
| T70 | 693.82 | 308.29 | 0.011532 | 26,733.44 |

**Table 3.** Transverse frame—comparison of the roof top displacements obtained by the proposed method and nonlinear direct dynamic analysis.

| Earthquake | Rigid Connect. (1) | Proposed Model (2) | Nonlinear Dynamics (3) | (3)/(2) | (2)/(1) |
|---|---|---|---|---|---|
| Ulcinj–Albatros | 0.0901 m | 0.1504 m | 0.1539 m | 1.0233 | 1.6693 |
| El Centro | 0.1099 m | 0.1287 m | 0.1242 m | 0.9650 | 1.1711 |

**Table 4.** Longitudinal frame—comparison of the roof top displacements obtained by the proposed method and nonlinear direct dynamic analysis.

| Earthquake | Rigid Connect. (1) | Proposed Model (2) | Nonlinear Dynamics (3) | (3)/(2) | (2)/(1) |
|---|---|---|---|---|---|
| Ulcinj–Albatros | 0.0787 m | 0.1137 m | 0.1168 m | 1.0273 | 1.4447 |
| El Centro | 0.0877 m | 0.1022 m | 0.0931 m | 0.9109 | 1.1653 |

## 4. Results and Discussion

Behavior of the experimental models EM-1 and EM-2 has shown that the connection between the corner column and floor beam possesses great rotation capacity. The yielding phase occurs due to significant displacements ranging from ±30 to ±40 mm. In the final phase, the structural connection shows a tendency to harden. Failure occurs when the tenon begins to separate from the beam, as shown in Figure 5c. This connection was tested by applying a relatively small axial pressure force, and therefore, the registered hysteresis dependence is valid for such conditions in practice. The beam is to be treated as a partially fixed element with nonlinear bearing characteristics of the connection. Taking such behavior of this connection into consideration, there is a real danger of bond slippage of the tenon from the column during a strong earthquake due to out-of-phase vibrations. Therefore, it is necessary to provide a real simulation of its experimentally proven nonlinear characteristics in all further analytical considerations.

A certain level of rigidity of connection of floor structure elements K-45 with the girder, labeled as EM-3 and EM-4, is achieved by a reinforced finishing concrete layer. Such a structural solution enables transmission of negative moments. Nonlinear characteristics of this connection are presented as half-hysteretic relations: force–displacement and moment–rotation. After reaching the limit bearing force, for each subsequent loading and unloading cycle, there is a sudden drop in the bearing force. After decreasing, the load-bearing limit force of this connection remains at the level of about 1/3 of the maximum registered load-bearing limit force, that is, until the occurrence of brittle fracture.

Test of the model EM-5 shows that the foundation is very favorable and it does not experience any damage. Column inclination occurs above the pocket foundation with corresponding propagation of plastic hinge, which is favorable. Nonlinear hysteretic relations for the critical cross-section of the column in the form of force–displacement and moment–rotation, as shown in Figure 17, show very stable nonlinear characteristics and a high level of ductility, which is very favorable for the integral structural system.

The test results of model EM-6 show that a successful structural solution (with adequate reinforcing of the reduced cross-section of the column by longitudinal bars) is created at the point of the weakened column, which enables very stable behavior of this connection. Characteristics of the nonlinear behavior of the weakened and full cross-sections of the column are very close, i.e., deviation is almost negligible, which confirms the quality of this connection.

The validation of the proposed approach for the calculation of the displacements using material linear direct dynamic analysis and reduced stiffness calculated based on the bending moments on the frame with rigid joints, and experimentally/theoretically defined

moment–rotation relationships of connections is conducted comparing the results with the materially nonlinear direct dynamic analysis of the same frames (previous research, Ref. [55]). The nonlinear direct dynamic analysis was conducted using the finite element method and the program NORA 2005 [56]. The material nonlinearity was simulated by applying a dense subdivision of the elements into a series of closely spaced cross-sections whose constitutive relations were represented by M–φ.

Comparing the roof top displacements obtained by the proposed approach and nonlinear direct dynamic analysis, shown in Tables 3 and 4, it can be concluded that the proposed model provides reliable results considering that the differences are in the range of 2.33–8.91%. Accordingly, the proposed model has been validated for application in everyday engineering practice, being significantly simpler to implement compared to direct dynamic analysis, in cases where experimental data on connection capacity or theoretical relationships are available.

The differences in the roof top displacements of the analyzed frames under the considered earthquake excitations between the proposed model and the model with the rigid joints, shown in Tables 3 and 4, are in the range from 16.53% to 66.93%. These results confirm the necessity of considering the nonlinear behavior and stiffness of connections in precast frame structures when determining displacements, which is particularly important for the verification of the serviceability limit state of structures in seismic regions.

The inter-story drift ratios at time of maximum roof top displacement calculated using the proposed model are analyzed and compared with the case of rigid connections, as well (Figures 26 and 27). It can be concluded that connection stiffness significantly influences the seismic response of precast frame structures. Namely, under the Ulcinj–Albatros earthquake, the inter-story drift ratio at the ground floor for the case of semi-rigid connections is larger for approx. 100% and 80% compared to the case of rigid connections for transverse and longitudinal frames, respectively. On the first floor, inter-story drift ratios are larger for approx. 25% and 10%. It should be mentioned that the maximum inter-story drift ratio is larger at the first floor in the case of rigid connections, while it is larger at the ground floor in the case of semi-rigid connections. Furthermore, the inter-story drift ratios are compared with the limit value according to the standard EN 1998-1 [49] for buildings in which non-structural elements are fixed so that they do not interfere with structural deformations (1%). For almost all the analyzed cases of frames with rigid connections, drifts are slightly lower or slightly higher than the limit value. On the other hand, in cases of frames with semi-rigid connections, reals stiffnesses, drifts are significantly larger than the limit value, which confirms the necessity of considering the nonlinear behavior and stiffness of connections in precast frame structures, especially for the seismic vulnerability of existing structures.

The obtained results regarding the roof top displacements and inter-story drift ratios are fully in accordance with previous research. Ingle et al. [36] analyzed the seismic response of a 10-story precast concrete building frame with 12 types of modeling of the beam–column joints under seven earthquake records. They concluded that the peak top displacements are significantly larger (from approx. 10% to 200% regarding the connection modeling type) compared to the case of a monolithic frame. Comparable results are reported in [57] as well. Song et al. [17] analyzed an eight-story two-bay frame with six different variants of the connections and compared the results with the monolithic counterpart and concluded that under strong seismic excitation, the response differences between precast frames and the RC frame were significant (approx. 10–30% regarding the inter-story drift ratios), so it is worthwhile to appropriately incorporate connections behavior and stiffness in precast frames seismic analysis.

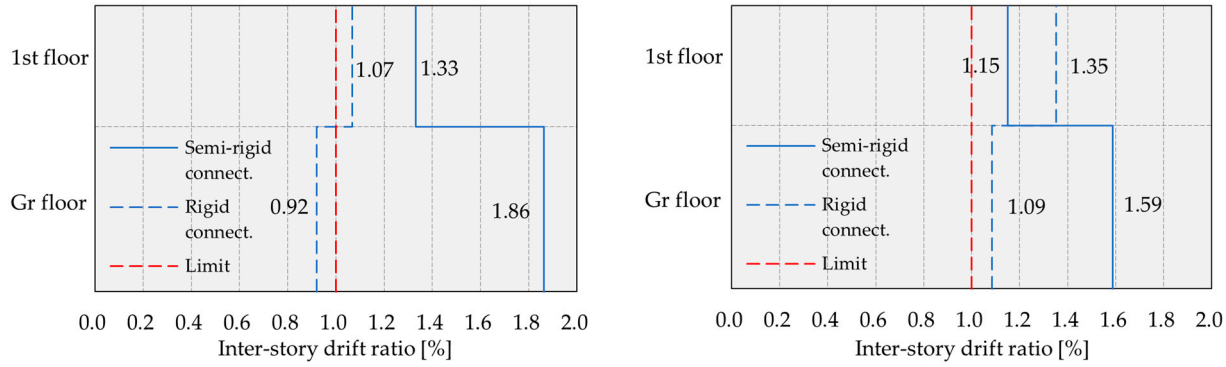


**Figure 26.** Inter-story drift ratio—transverse frame: (**a**) Ulcinj–Albatros (N–S component); (**b**) El Centro (S00E component).

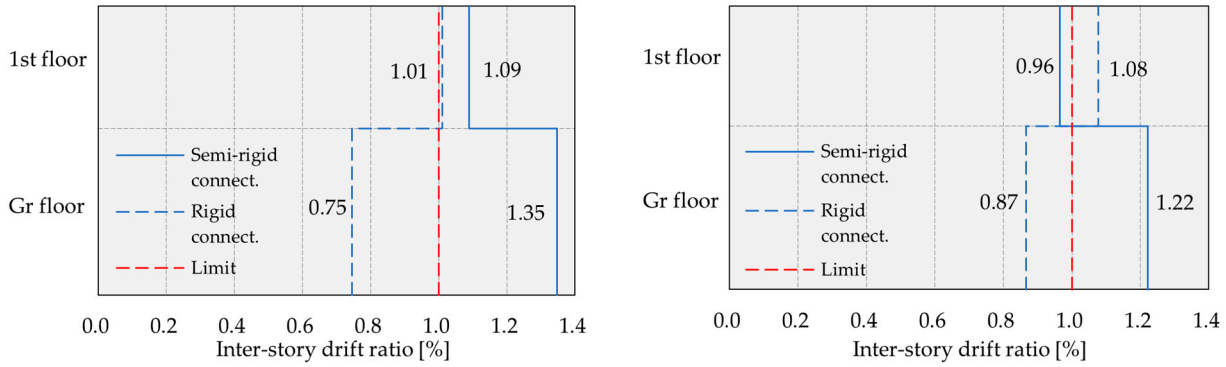


**Figure 27.** Inter-story drift ratio—longitudinal frame: (**a**) Ulcinj–Albatros (N–S component); (**b**) El Centro (S00E component).

## 5. Conclusions

Based on the experimental research of the precast frame element connection capacity of one characteristic industrial hall chosen as the case study and the proposed numerical analysis for seismic response regarding structural displacements, the following conclusions can be drawn:

1. All the experimentally tested connection overlays showed satisfying nonlinear behavior with certain specifics regarding failure. The connection of the floor beam to the corner column is prone to the bond slippage of the tenon from the column during a strong earthquake. The connection of the floor element with the floor beam is characterized by a reduction in the resistance up to 60% after the load-bearing limit force, which can be characterized as brittle fracture. The column–foundation connection and the weakened column–floor beam connection showed stable nonlinear hysteretic behavior with slight stiffness degradation after reaching the ultimate load-bearing capacity, which can be accepted as favorable in the seismic-prone regions.
2. These results confirm the necessity of considering the nonlinear behavior and stiffness of connections in precast frame structures when determining displacements, which is particularly important for the verification of the serviceability limit state of structures in seismic regions.
3. The simplified approach for taking into account stiffness reduction due to nonlinear behavior of element connections is proposed in the paper.

4. The proposed model is validated considering that the roof top displacements differ in the range of 2.33–8.91% compared to nonlinear direct dynamic analysis results.
5. Roof top displacements of the considered structure are larger by 16.53–66.93% when the stiffness of the connections is taken into account, compared to the case where the connections are treated as rigid. In the case of inter-story drift ratios, the values are larger by 10–100%, highlighting that inter-story drift ratios are larger than the limit value provided by standard EN 1998-1 when the real stiffnesses of connections are considered. This is especially important from the aspect of the serviceability limit state of structures in seismic regions.
6. The simplified approach and proposed modeling of the connections are applicable for seismic risk assessment of existing industrial halls and commercial buildings constructed in the considered structural system, and for other PCR systems which are produced industrially in large series and which are designed in zones of seismic activity VIII or IX.

**Author Contributions:** Conceptualization, B.M. (Biljana Mladenović), D.Z. and D.R.; methodology, B.M. (Biljana Mladenović) and J.R.; software, A.Z., B.M. (Bojan Milošević) and K.S.; validation, B.M. (Biljana Mladenović), A.Z., D.Z., D.R., J.R., B.M. (Bojan Milošević) and K.S.; formal analysis, A.Z. and J.R.; investigation, B.M. (Biljana Mladenović), D.Z. and D.R.; resources, B.M. (Biljana Mladenović) and B.M. (Bojan Milošević); data curation, D.Z., D.R. and J.R.; writing—original draft preparation, B.M. (Biljana Mladenović), A.Z., B.M. (Bojan Milošević) and K.S.; writing—review and editing, D.Z., D.R. and J.R.; visualization, B.M. (Biljana Mladenović) and A.Z.; supervision, D.Z. and D.R.; project administration, B.M. (Biljana Mladenović) and B.M. (Bojan Milošević); funding acquisition, D.Z. All authors have read and agreed to the published version of the manuscript.

**Funding:** This research was supported by the Ministry of Science, Technological Development and Innovation of the Republic of Serbia, under the Agreement on Financing the Scientific Research Work of Teaching Staff at the Faculty of Mechanical Engineering and Civil Engineering in Kraljevo, University of Kragujevac—Registration number: 451-03-137/2025-03/200108 and at the Faculty of Civil Engineering and Architecture, University of Nis—Registration number: 451-03-137/2025-03/200095 dated 4 February 2025.

**Data Availability Statement:** The data presented in this study are available on request from the corresponding author. The data are not publicly available due to privacy concerns.

**Conflicts of Interest:** The authors declare no conflicts of interest.

## References

1. Ristic, D. *Observed Damage Industrial Structures Due to Friuli, Italy Earthquake of 1976*; IZIIS-Skopje: Skopje, North Macedonia, 1976.
2. Marzo, A.; Marghella, G.; Indirli, M. The Emilia-Romagna earthquake: Damages to precast/prestressed reinforced concrete factories. *Ing. Sismica* **2012**, *30*, 132–147. Available online: https://www.researchgate.net/publication/259911421 (accessed on 5 November 2025).
3. Avğın, S.; Köse, M.M.; Çınar, M. Critical review of design practices and observed damages in precast industrial buildings: Evidence from the February 2023 Türkiye earthquakes. *Bull. Earthq. Eng.* **2025**. [CrossRef]
4. Maeda, M.; Al-Washali, H. Damage Due to Earthquakes and Improvement of Seismic Performance of Reinforced Concrete Buildings in Japan. In *Seismic Hazard and Risk Assessment*; Vacareanu, R., Ionescu, C., Eds.; Springer Natural Hazards; Springer: Cham, Switzerland; London, UK, 2018; pp. 361–372. [CrossRef]
5. Blakeborough, A.; Merriman, P.A.; Williams, M.S. (Eds.) *The Northridge California Earthquake of 17 January 1994, a Field Report by EEFIT*; Institution of Structural Engineers: London, UK, 1994; Available online: https://www.eeri.org/1994/01/northridge-california/ (accessed on 1 November 2025).
6. Muguruma, H.; Nishiyama, M.; Watanabe, F. Lessons learned from the Kobe earthquake, A Japanese perspective. *PCI J.* **1995**, *40*, 28–42. [CrossRef]

7. Posada, M.; Wood, S.L. Seismic performance of precast industrial buildings in Turkey. In Proceedings of the Seventh U.S. National Conference on Earthquake Engineering, Boston, MA, USA, 21–25 July 2002.
8. Zhao, B.; Taucer, F.; Rossetto, T. Field investigation on the performance of building structures during the 12 May 2008 Wenchuan earthquake in China. *Eng. Struct.* **2009**, *31*, 1707–1723. [CrossRef]
9. Senel, S.M.; Kayhan, A.H. Fragility based damage assessment in existing precast industrial buildings: A case study for Turkey. *Struct. Eng. Mech.* **2010**, *34*, 39–60. [CrossRef]
10. Nikolić-Brzev, S.; Marko Marinković, M.; Ivan Milićević, I.; Blagojević, N.; Isufi, B. *Consequences of the Earthquake in Albania from November 26, 2019 on Facilities and Infrastructure*; Serbian Association for Earthquake Engineering; Akademska misao: Belgrade, Serbia, 2020; ISBN 978-86-7466-843-6. (In Serbian)
11. Kurama, Y.C.; Sritharan, S.; Fleischman, R.B.; Restrepo, J.I.; Henry, R.S.; Cleland, N.M.; Ghosh, S.K.; Bonelli, P. Seismic-Resistant Precast Concrete Structures: State of the Art. *J. Struct. Eng.* **2018**, *144*, 03118001. [CrossRef]
12. Sucuoglu, H. Effect of connection rigidity on seismic response of precast concrete frames. *PCI J.* **1995**, *40*, 94–103. [CrossRef]
13. Zlatkov, D.; Zdravković, S.; Mladenović, B.; Mijalković, M. Seismic analysis of frames with semi-rigid connections in accordance with EC8. *Facta Univ. Ser. Archit. Civ. Eng.* **2020**, *18*, 203–217. [CrossRef]
14. Elliott, K.S.; Davies, G.; Ferreira, M.; Gorgun, H.; Mahdi, A.A. Can precast concrete structures be designed as semi rigid frames? Part 1—The experimental evidence. *Struct. Eng.* **2003**, *81*, 14–27.
15. Pampanin, S.; Priestley, M.J.N.; Sritharan, S. Analytical modelling of the seismic behaviour of precast concrete frames designed with ductile connections. *J. Earthq. Eng.* **2001**, *5*, 329–368. [CrossRef]
16. Kremmyda, G.D.; Fahjan, Y.M.; Psycharis, I.N. Analytical prediction of the shear resistance of precast RC pinned beam-to-column connections. In Proceedings of the 4th ECCOMAS Thematic Conference on Computational Methods in Structural Dynamics and Earthquake Engineering (COMPDYN 2013), Kos Island, Greece, 12–14 June 2013; pp. 1502–1514.
17. Song, B.; Du, D.; Li, W.; Wang, S.; Wang, Y.; Feng, D. Analytical investigation of the differences between cast-in-situ and precast beam-column connections under seismic actions. *Appl. Sci.* **2020**, *10*, 8280. [CrossRef]
18. Guerrero, H.; Rodriguez, V.; Escobar, J.A.; Alcocer, S.M.; Bennetts, F.; Suarez, M. Experimental tests of precast reinforced concrete beam-column connections. *Soil Dyn. Earthq. Eng.* **2019**, *124*, 105743. [CrossRef]
19. Nascimbene, R.; Bianco, L. Cyclic response of column to foundation connections of reinforced concrete precast structures: Numerical and experimental comparisons. *Eng. Struct.* **2021**, *247*, 113214. [CrossRef]
20. Hemamathi, L.; Jaya, K.P. Behaviour of precast column foundation connection under reverse cyclic loading. *Adv. Civ. Eng.* **2021**, *2021*, 6677007. [CrossRef]
21. Fischinger, M.; Zoubek, B.; Isaković, T. Seismic Response of Precast Industrial Buildings. In *Perspectives on European Earthquake Engineering and Seismology*; Ansal, A., Ed.; Springer: Cham, Switzerland, 2014; Volume 34, pp. 67–87. [CrossRef]
22. Kremmyda, G.D.; Fahjan, Y.M.; Tsoukantas, S.G. Nonlinear FE analysis of precast RC pinned beam-to-column connections under monotonic and cyclic shear loading. *Bull. Earthq. Eng.* **2014**, *12*, 1615–1638. [CrossRef]
23. Kremmyda, G.D.; Fahjan, Y.M.; Psycharis, I.N.; Tsoukantas, S.G. Numerical investigation of the resistance of precast RC pinned beam-to-column connections under shear loading. *Earthq. Eng. Struct. Dyn.* **2017**, *46*, 1511–1529. [CrossRef]
24. Zoubek, B.; Fahjan, Y.M.; Fischinger, M.; Isaković, T. Nonlinear finite element modelling of centric dowel connections in precast buildings. *Comput. Concr.* **2014**, *14*, 463–477. [CrossRef]
25. Zoubek, B.; Fischinger, M.; Isakovic, T. Estimation of the cyclic capacity of beam-to-column dowel connections in precast industrial buildings. *Bull. Earthq. Eng.* **2015**, *13*, 2145–2168. [CrossRef]
26. Feng, D.-C.; Wu, G.; Lu, Y. Finite element modelling approach for precast reinforced concrete beam-to-column connections under cyclic loading. *Eng. Struct.* **2018**, *174*, 49–66. [CrossRef]
27. Sousa, R.; Batalha, N.; Rodrigues, H. Numerical simulation of beam-to-column connections in precast reinforced concrete buildings using fibre-based frame models. *Eng. Struct.* **2020**, *203*, 109845. [CrossRef]
28. Tarabia, A.M.; Etman, E.E.; Allam, S.M.; Aboelhassan, M.G. Modeling of precast reinforced concrete beam-column joints under cyclic loading. *J. Earthq. Eng.* **2022**, *26*, 7626–7655. [CrossRef]
29. Hawileh, R.A.; Rahman, A.; Tabatabai, H. Nonlinear finite element analysis and modeling of a precast hybrid beam-column connection subjected to cyclic loads. *Appl. Math. Model.* **2010**, *34*, 2562–2583. [CrossRef]
30. Ozden, S.; Ertas, O. Modeling of pre-cast concrete hybrid connections by considering the residual deformations. *Int. J. Phys. Sci.* **2010**, *5*, 781–792.
31. Nzabonimpa, J.D.; Hong, W.-K.; Kim, J. Nonlinear finite element model for the novel mechanical beam-column joints of precast concrete-based frames. *Comput. Struct.* **2017**, *182*, 129–143. [CrossRef]

32. Kataoka, M.N.; Ferreira, M.A.; El Debs, A.L.H.C. Nonlinear FE analysis of slab-beam-column connection in precast concrete structures. *Eng. Struct.* **2017**, *143*, 306–315. [CrossRef]
33. Brunesi, E.; Nascimbene, R.; Bolognini, D.; Bellotti, D. Experimental investigation of the cyclic response of reinforced precast concrete framed structures. *PCI J.* **2015**, *60*, 57–79. [CrossRef]
34. Xue, W.; Yang, X. Seismic tests of precast concrete, moment-resisting frames and connections. *PCI J.* **2010**, *55*, 102–121. [CrossRef]
35. Chourasia, A.; Kajale, Y.; Singhal, S.; Parashar, J. Seismic performance assessment of two-storey precast reinforced concrete building. *Struct. Concr.* **2020**, *21*, 2011–2027. [CrossRef]
36. Ingle, A.S.; Bharti, S.D.; Shrimali, M.K.; Datta, T.K. Modeling of Precast Building Frames for Seismic Response Analysis. *J. Vib. Eng. Technol.* **2024**, *12*, 8419–8436. [CrossRef]
37. Wang, Z.; Feng, D.-C.; Cao, X.; Wu, G. Seismic performance assessment of code-conforming precast reinforced concrete frames in China. *Earthq. Struct.* **2021**, *21*, 277–289. [CrossRef]
38. Magliulo, G.; Bellotti, D.; Cimmino, M.; Nascimbene, R. Modeling and Seismic Response Analysis of RC Precast Italian Code-Conforming Buildings. *J. Earthq. Eng.* **2018**, *22*, 140–167. [CrossRef]
39. Bressanelli, M.E.; Belleri, A.; Riva, P.; Magliulo, G.; Bellotti, D.; Dal Lago, B. Effects of modeling assumptions on the evaluation of the local seismic response for RC precast industrial buildings. In Proceedings of the 7th ECCOMAS Thematic Conference on Computational Methods in Structural Dynamics and Earthquake Engineering (COMPDYN 2019), Crete, Greece, 24–26 June 2019; pp. 182–195.
40. Rodrigues, H.; Vitorino, H.; Batalha, N.; Sousa, R.; Fernandes, P.; Varum, H. Influence of Beam-to-Column Connections in the Seismic Performance of Precast Concrete Industrial Facilities. *Struct. Eng. Int.* **2022**, *32*, 507–519. [CrossRef]
41. Bressanelli, M.E.; Bellotti, D.; Belleri, A.; Cavalieri, F.; Riva, P.; Nascimbene, R. Influence of Modelling Assumptions on the Seismic Risk of Industrial Precast Concrete Structures. *Front. Built Environ.* **2021**, *7*, 629956. [CrossRef]
42. Bosio, M.; Di Salvatore, C.; Bellotti, D.; Capacci, L.; Belleri, A.; Piccolo, V.; Cavalieri, F.; Dal Lago, B.; Riva, P.; Magliulo, G.; et al. Modelling and seismic response analysis of nonresidential single-storey existing precast buildings in Italy. *J. Earthq. Eng.* **2022**, *27*, 1047–1068. [CrossRef]
43. Bosio, M.; Labò, S.; Riva, P.; Belleri, A. Seismic risk and finite element modelling influence of an existing one-storey precast industrial building. *J. Earthq. Eng.* **2023**, *27*, 4182–4205. [CrossRef]
44. Batalha, N.; Rodrigues, H.; Sousa, R.; Varum, H. Seismic assessment of existing precast RC industrial buildings in Portugal. *Struct.* **2022**, *41*, 777–786. [CrossRef]
45. Ristic, D.; Micov, V.; Zisi, N.; Dimitrovski, T.; Zdravkovic, S. *Attesting of Static and Seismic Stability of Typified Moduli of the Hall Programme of Precast RC Structural System "AMONT", Krusce: Volume II: Quasi-Static Testing of Bearing and Deformability Chracteristics up to Failure of Characteristic Full-Scale Models of Joints of "AMONT" System*; IZIIS Report 98-37; Institute of Earthquake Engineering and Engineering Seismology (IZIIS): Skopje, North Macedonia, 1998.
46. Ristic, D.; Sesov, N.; Zisi, N.; Micov, V.; Zdravkovic, S. *Attesting of Static and Dynamic Stability of Typified Modules of Hall Programme of Precast RC Structural System "AMONT", Krusce: Volume IV: Attesting Analysis of Nonlinear Dynamic Behaviour of Two-Storey Hall in AMONT System under Effect of Actual Earthquakes by Application of Verified Completely Nonlinear Model*; IZIIS Report 98-39; Institute of Earthquake Engineering and Engineering Seismology (IZIIS): Skopje, North Macedonia, 1998.
47. Ivanov, I.; Velchev, D. Comparative Study of Different Linear Analysis for Seismic Resistance of Buildings According to Eurocode 8. *Vibration* **2025**, *8*, 21. [CrossRef]
48. Meral, E.; Cayci, B.T.; Inel, M. Comparative Study on the Linear and Nonlinear Dynamic Analysis of Typical RC Buildings. *Rev. Constr.* **2024**, *23*, 587. [CrossRef]
49. *EN 1998-1:2005*; Eurocode 8: Design of Structures for Earthquake Resistance—Part 1: General Rules, Seismic Actions and Rules for Buildings. CEN: Brussels, Belgium, 2005.
50. *EN 1992-1-1:2004*; Eurocode 2: Design of Concrete Structures—Part 1-1: General Rules and Rules for Buildings. CEN: Brussels, Belgium, 2004.
51. ACI Committee 318. *Building Code Requirements for Structural Concrete (ACI 318-19)*; American Concrete Institute: Farmington Hills, MI, USA, 2019.
52. American Society of Civil Engineers (ASCE). *Minimum Design Loads and Associated Criteria for Buildings and Other Structures (ASCE/SEI 7-22)*; ASCE: Reston, VA, USA, 2022.
53. Computers and Structures Inc. *CSI Analysis Reference Manual*; Computers and Structures Inc.: Berkley, CA, USA, 2016.
54. Zorić, A.; Zlatkov, D.; Trajković-Milenković, M.; Vacev, T.; Petrović, Ž. Analysis of the seismic response of an RC frame structure with lead rubber bearings. *Build. Mater. Struct.* **2022**, *65*, 73–80. [CrossRef]
55. Zlatkov, D. Theoretical and Experimental Analysis of Reinforced Concrete Frame Structures with Semi-Rigid Connections. Ph.D. Thesis, University of Niš, Niš, Serbia, 2015. (In Serbian)

56. Ristic, D. Nonlinear Behaviour and Stress-Strain Based Modeling of Reinforced Concrete Structures Under Eartquake Induced Bending and Varying Axial Loads. Ph.D. Thesis, School of Civil Engineering, Kyoto University, Kyoto, Japan, June 1988.
57. Low, S.-G.; Tadros, M.K.; Einea, A.; Magaña, R.A. Seismic Behavior of a Six-Story Precast Concrete Office Building. *PCI J.* **1996**, *41*, 56–77. [CrossRef]